

Olivine-wadsleyite transition in the system (Mg,Fe)₂SiO₄

Tomoo Katsura, Hitoshi Yamada,¹ Osamu Nishikawa,² Maoshuang Song, Atsushi Kubo,³ Toru Shinmei,⁴ Sho Yokoshi, Yoshitaka Aizawa, Takashi Yoshino,⁵ Michael J. Walter, and Eiji Ito

Institute for Study of the Earth's Interior, Okayama University, Misasa, Japan

Ken-ichi Funakoshi

Japan Synchrotron Radiation Research Institute, Kouto, Japan

Received 7 February 2003; revised 24 October 2003; accepted 21 November 2003; published 25 February 2004.

[1] Phase relations of the olivine-wadsleyite transition in the system (Mg,Fe)₂SiO₄ have been determined at 1600 and 1900 K using the quench method in a Kawai-type high-pressure apparatus. Pressure was determined at a precision better than 0.2 GPa using in situ X-ray diffraction with MgO as a pressure standard. The transition pressures of the end-member Mg₂SiO₄ are estimated to be 14.2 and 15.4 GPa at 1600 and 1900 K, respectively. Partition coefficients for Fe and Mg between olivine and wadsleyite are 0.51 at 1600 K and 0.61 at 1900 K. By comparing the depth of the discontinuity with the transition pressure, the temperature at 410 km depth is estimated to be 1760 ± 45 K for a pyrolitic upper mantle. The mantle potential temperature is estimated to be in the range 1550–1650 K. The temperature at the bottom of the upper mantle is estimated to be 1880 ± 50 K. The thickness of the olivine-wadsleyite transition in a pyrolitic mantle is determined to be between 7 and 13 km for a pyrolitic mantle, depending on the efficiency of vertical heat transfer. Regions of rapid vertical flow (e.g., convection limbs), in which thermal diffusion is negligible, should have a larger transition interval than stagnant regions, where thermal diffusion is effective. This is in apparent contradiction to short-period seismic wave observations that indicate a maximum thickness of <5 km. An upper mantle in the region of the 410 km discontinuity with about 40% olivine and an Mg# of at least 89 can possibly explain both the transition thickness and velocity perturbation at the 410 km discontinuity.

INDEX TERMS: 3630 Mineralogy and Petrology: Experimental mineralogy and petrology; 3924 Mineral Physics: High-pressure behavior; 7207 Seismology: Core and mantle; 7218 Seismology: Lithosphere and upper mantle; 8124 Tectonophysics: Earth's interior—composition and state (1212); **KEYWORDS:** olivine-wadsleyite transition, 410 km discontinuity, phase relations, mantle geotherm, composition of the mantle

Citation: Katsura, T., et al. (2004), Olivine-wadsleyite transition in the system (Mg,Fe)₂SiO₄, *J. Geophys. Res.*, 109, B02209, doi:10.1029/2003JB002438.

1. Introduction

[2] Seismological studies show abrupt increases in seismic wave velocities near a depth of 410 km in the Earth's mantle, appropriately called the 410 km discontinuity [cf. *Shearer*, 2000]. The 410 km discontinuity is usually attributed to the olivine-wadsleyite transition in a pyrolitic mantle

composition [*Ringwood*, 1979]. Hence to understand this discontinuity requires accurate and precise knowledge of olivine-wadsleyite transition in the system (Mg,Fe)₂SiO₄, and many workers have studied this transition extensively [cf. *Katsura and Ito*, 1989; *Akaogi et al.*, 1989].

[3] Temperature is one of the most important parameters for modeling the dynamics of the Earth's interior. Previous studies indicate that the olivine-wadsleyite transition pressure has some temperature dependence. Therefore upper mantle temperature can be estimated by comparing the depth of the discontinuity with the transition pressure. Temperature estimation in this way is of primary importance, because presently there is essentially no other method for estimating temperature in the deep mantle.

[4] *Katsura and Ito* [1989] and *Fei and Bertka* [1999] carried out phase equilibrium experiments in (Mg,Fe)₂SiO₄ using a conventional Kawai-type high-pressure apparatus, in which pressures were estimated by calibration against

¹Now at City Hall of Nagahama, Nagahama, Japan.

²Now at Department of Earth Sciences, Faculty of Science, Kanazawa University, Kanazawa, Japan.

³Now at Department of Geosciences, Princeton University, Princeton, New Jersey, USA.

⁴Now at Geodynamics Research Center, Ehime University, Matsuyama, Japan.

⁵Now at Department of Earth and Environmental Sciences, Rensselaer Polytechnic Institute, Troy, New York, USA.

press load. However, this kind of ex situ pressure calibration will have considerable uncertainty. One reason is that generated pressure is sensitive to the heating path, and actual pressure may vary from run to run even at constant press load. Consequently, transition pressures reported by *Katsura and Ito* [1989] and *Fei and Bertka* [1999] or based on thermochemical calculations by *Akaogi et al.* [1989], which are in turn based on externally calibrated high-pressure experiments, are not sufficiently precise for reliable estimation of upper mantle temperature.

[5] *Morishima et al.* [1994] determined the phase boundary of the olivine-wadsleyite transition in Mg_2SiO_4 by means of in situ X-ray diffraction in a cubic anvil apparatus. In this method, sample pressure is determined precisely by measuring the volume change of a reference material. However, while establishing an important end-member baseline, *Morishima et al.*'s [1994] results cannot be directly used to estimate temperature in the mantle because of the absence of iron. Thus it is necessary to determine phase relations of the olivine-wadsleyite transition in the binary $(\text{Mg,Fe})_2\text{SiO}_4$ system by means of in situ pressure determination by X-ray diffraction.

[6] In addition to depth, the sharpness of the discontinuity gives important information about the deep mantle that must also be consistent with the phase relations. Recent developments in seismology have made it possible to detect various kinds of reflected and converted waves from the 410 km discontinuity. Reflected and converted phases of short period (~ 1 Hz) P waves have been detected [*Benz and Vidale*, 1993; *Yamazaki and Hirahara*, 1994; *Neele*, 1996], and these observations suggest that the 410 km discontinuity is very sharp. The thickness of a discontinuity must be less than half of the wavelength to generate an observable reflection wave [*Helffrich and Bina*, 1994], and the thickness of the 410 km discontinuity is considered to be less than 5 km [*Shearer*, 2000].

[7] *Katsura and Ito* [1989] predicted that the thickness of the olivine-wadsleyite transition should be 11–19 km in a pyroclitic mantle, which is inconsistent with seismic observations. *Stixrude* [1997] presented one way to reconcile the seismic observations with the phase relations by taking into account the nonideality of the wadsleyite yielding rate, as well as the effects of Fe-Mg partitioning among coexisting mantle minerals on the thickness of the transition. However, the interval of the binary loop is temperature-dependent, and temperatures higher than 2100 K are necessary for this kind of reconciliation. Estimates of upper mantle potential temperature of about 1600 K based on mid-ocean ridge basalt (MORB) chemistry [*McKenzie and Bickle*, 1988], make such high temperatures at the 410 km discontinuity unlikely.

[8] *Helffrich and Wood* [1996] suggested that if the shape of the olivine-wadsleyite loop were that of an upward crescent, then the transition interval could be much smaller than *Katsura and Ito*'s [1989] estimation. As mentioned above, the precision of experimental pressures given by *Katsura and Ito* [1989] is fairly low, no better than 0.5 GPa, so the precise shape of the loop has to be determined.

[9] The purpose of this study is to determine the phase relations of the olivine-wadsleyite transition in the system $(\text{Mg,Fe})_2\text{SiO}_4$ more accurately and precisely than given by our previous study [*Katsura and Ito*, 1989]. We determined the phase relations using a combination of pressure deter-

mination by in situ X-ray diffraction and compositional measurement by electron microprobe. The resulting phase relations are used to refine estimates for upper mantle temperature and to place tighter constraints on predicted transition thickness as a function of mantle composition.

2. Experimental Procedure

2.1. In Situ X-Ray Diffraction

[10] High P - T in situ X-ray diffraction experiments were conducted at the third generation synchrotron radiation facility "SPring-8" in Hyogo prefecture, Japan. For high-pressure and high-temperature generation, we used a Kawai-type apparatus, "SPEED-1500," installed at a white X-ray bending magnet beam line BL04B1 [*Utsumi et al.*, 1998]. Energy-dispersive X-ray diffraction was conducted using a horizontal goniometer. The vertical and horizontal widths of incident slits were 0.1 and 0.05 mm, respectively. The horizontal width of the dispersion and receiving slits were 0.05 and 0.2 mm. A Ge solid-state detector was used and connected to a multichannel analyzer with 4096 channels, which was calibrated using characteristic X rays of Cu, Mo, Ag, Ta, Pt, Au and Pb. Exposure times were usually 200–300 s. The energy range available for analyzing the sample was ~ 40 –140 keV, and the diffraction angle (2θ) was $\sim 6^\circ$.

[11] We used MgO as a pressure standard because its thermoelastic properties have been studied extensively. MgO has a simple cubic structure (NaCl structure), and no solid phase transitions are known at any P - T condition. It has a very high melting point even at ambient pressure (3100 K), and therefore, can be used as a pressure standard at very high temperatures. We used at least 4 diffraction lines, i.e., (111), (200), (220), (311), (222), and (400) to determine unit cell volume at high P - T conditions. When observed, we also used one or more of the (331), (511), (440), (442), (444), and (531) lines. Errors in pressure arising from peak fitting are about ± 0.1 GPa. In order to minimize systematic errors, we calibrated 2θ before and after each run using sintered MgO at ambient condition by matching the observed unit cell parameter to the value given by the JCPDS card ($a_0 = 4.2112$ Å). Errors from the 2θ calibration are about ± 0.05 GPa.

[12] For calculating pressure, we used the equation of state (EoS) of MgO proposed by *Matsui et al.* [2000] (Matsui scale), which is based on an MD simulation with breathing model. The Matsui scale is considered to be reliable because it reproduces important experimental thermoelastic data: volume at ambient condition, compression at ambient temperature, thermal expansion at ambient pressure, and bulk modulus at high temperature and ambient pressure. Moreover, *Matsui and Nishiyama* [2002] demonstrated that the pressure of the postspinel transition can be reconciled with the depth of 660 km discontinuity by using the Matsui scale, although there is a discrepancy when using *Anderson et al.*'s [1989] EoS of gold [*Irfune et al.*, 1998; *Katsura et al.*, 2003].

[13] We also used the EoS of MgO proposed by *Speziale et al.* [2001] (Speziale scale) for comparison. We obtained 0.15 \sim 0.17 GPa lower pressure using the Speziale scale relative to the Matsui scale. *Jamieson et al.* [1982] and *Hama and Suito* [1999] also proposed EoSs of MgO. These two EoSs, however, do not duplicate data of thermal

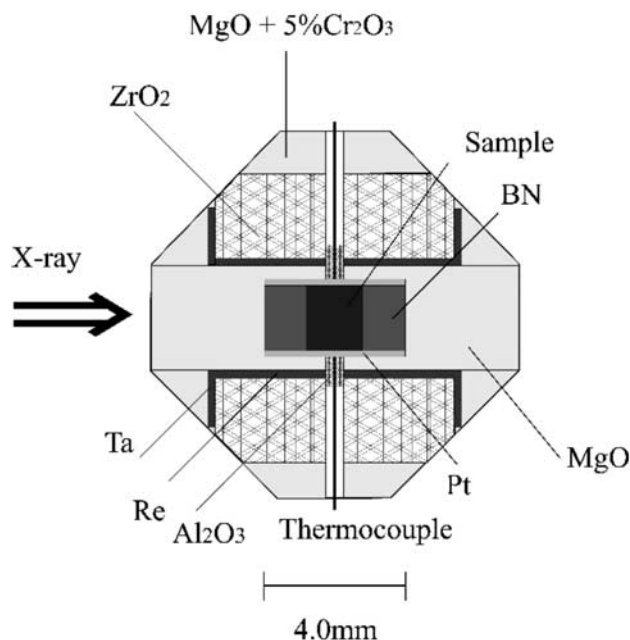


Figure 1. Horizontal cross section of the sample assembly. The furnace system essentially has a cylindrical geometry in the horizontal direction of the drawing. The incident X rays go through the sample almost parallel to the furnace axis.

expansion at ambient pressure [Suzuki, 1975], and, consequently we chose not to use them for calculating pressure.

2.2. Sample Assembly for In Situ X-Ray Diffraction

[14] Starting materials were olivine solid solutions with compositions in $(\text{Mg}_x\text{Fe}_{1-x})_2\text{SiO}_4$, where $x = 0.97, 0.95, 0.93, 0.90, 0.85, 0.80$, and 0.70 . They were synthesized from Mg and Fe metals and tetraethylorthosilicate. Synthetic olivine powders were pressed into columns with 2 mm diameter, and sintered at 1670 K and ambient pressure for 10 min in a reduced gas flow with a ratio of $\text{H}_2:\text{CO}_2 = 1:1$. The sintered columnar samples were then ground into subcolumns with pie-shaped cross sections. The MgO pressure marker was obtained as a reagent, which was baked at 1700 K and ground into powder in a mortar. The MgO was mixed with boron nitride (BN) to suppress grain growth at high temperatures.

[15] The cross section of the cell assembly in a horizontal plane is schematically shown in Figure 1. The furnace system essentially has a cylindrical geometry, which is similar to our previous study on the postspinel transition in Mg_2SiO_4 [Katsura et al., 2003]. The furnace was a cylindrical Re heater with 3.0 mm in a length and 3.0 ϕ in an inner diameter. The heater was placed in a ZrO_2 thermal insulating sleeve. A Pt tube was loaded in the MgO container, which electrically insulated the heater and sample capsule. The temperature at the outside of the sample capsule was measured using a $\text{W}_{97}\text{Re}_3\text{-W}_{75}\text{Re}_{25}$ thermocouple, which is electrically insulated from the heater by Al_2O_3 sleeves.

[16] A cross section of the inside of the heater along a plane normal to the furnace axis is also shown Figure 2. Three or four separate olivine solid solutions were loaded into the Pt tube together with the MgO pressure marker. X

rays were irradiated almost parallel to the axis of the furnace system. By shifting the high-pressure apparatus, we can obtain diffraction patterns from each sample separately.

2.3. Run Procedure

[17] In this study we conducted a series of quench experiments with pressure measurement made by in situ X-ray diffraction. Phase relations were determined at 1600 and 1900 K, which are considered to be reasonable temperatures for the upper mantle.

[18] In initial runs, we first increased press load at ambient temperature, heated to a target temperature at constant press load, kept the temperature and press load for several tens of minutes, quenched the sample, and decompressed to ambient pressure. We found, however, that the generated pressure decreased by as much as a few GPa while keeping the temperature and press load constant. Such pressure drops are too large to construct precisely the olivine-wadsleyite two-phase loop, which is expected to be thinner than 1 GPa.

[19] In order to suppress such pressure drops, we adopted the following procedure. First, press load was increased to a value lower than the target load by 1 ~ 2 MN. At this load, the sample was heated to 1000 or 1100 K for 10 min for relaxation of pressure medium and gaskets. After that, the sample was cooled to ambient temperature, and recompressed to the target load. The sample was then heated to the target temperature within 15–25 min and maintained for 20–80 min. While keeping the temperature, the press load was successively increased by 0.5 ~ 2 MN to maintain constant sample pressure. Diffraction patterns of the pressure marker were successively acquired to monitor the generated pressure. Finally, the sample was quenched by cutting electrical current, and then decompressed to ambient conditions. This procedure was successful in limiting the pressure drop to ~0.2 GPa.

[20] Quenched samples were cut in a plane normal to the furnace axis, and made into polished cross sections. The

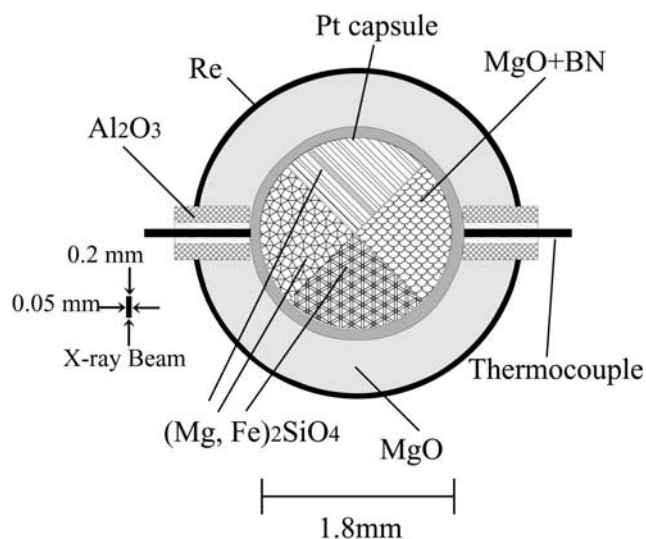


Figure 2. Cross section of the inside of the heater normal to the furnace axis. Three or four pieces of different olivine solid solution are loaded with the pressure marker parallel to the X-ray incidence.

Table 1. Results of In Situ X-Ray Experiments

	<i>T</i> , K	MgO, ^a <i>V</i> / <i>V</i> ₀	<i>P</i> , ^b GPa	Duration, min	Mg# _{Ol}	Mg# _{Wd}	<i>K</i> ^c
733	1900	0.9738 (6)	14.84 (18)	22	95.1 (5)	92.3 (1)	0.62 (7)
734	1900	0.9763 (3)	14.26 (15)	30	90.6 (5)	85.2 (7)	0.60 (5)
735	1900	0.9788 (3)	13.91 (15)	21	86.3 (9)	79.2 (3)	0.61 (5)
763	1600	0.9741 (5)	12.78 (17)	74	87.6 (6)	78.2 (6)	0.51 (3)
779	1600	0.9685 (5)	13.86 (17)	61	97.9 (3)	94.7 (6)	0.39 (7)
780	1600	0.9725 (6)	13.09 (18)	60	91.5 (6)	84.0 (4)	0.49 (4)

^aErrors in *V*/*V*₀ are from the pressure drift.^bErrors in pressure include those of the pressure drift, 2θ calibration, and temperature uncertainty.^c*K* = (100 − Mg#_{Ol}) Mg#_{Wd} / (100 − Mg#_{Wd}) Mg#_{Ol}.

sample section was examined by microfocused X-ray diffraction in our lab. The phases present were not easily distinguished by in situ X-ray diffraction in experiments at 1900 K. At high temperature, softening of the sample and pressure media causes grain growth of olivine and wadsleyite, which effectively decreased the number of subgrains in the limited diffraction area, preventing from observation of most diffraction lines.

[21] Quenched samples were also examined by scanning electron microscope, and in experiments with coexisting olivine and wadsleyite, phase compositions were measured by electron microprobe. No systematic variations were observed in the compositions of the coexisting phases of the sample. As is widely known, platinum tends to absorb iron from ferromagnesian silicates, and iron contents were lower in the grains located close (10 ~ 20 μm) to the platinum. Iron diffusion across the boundaries was observed between samples with different iron contents and between the sample and pressure marker. Phase compositions from these areas were not used to construct phase relations.

2.4. Supplemental Experiments

[22] In addition to in situ X-ray diffraction experiments, we have conducted several supplemental experiments to obtain reliable partition coefficients. As discussed below, the Fe-Mg partition coefficients obtained at 1600 K show a fair amount of scatter from run to run. In order to more precisely determine partition coefficient at 1600 K, we have conducted three additional experiments with the same sample assembly, in which pressure measurement was not conducted by in situ X-ray diffraction.

[23] Wadsleyite can be a solid solution in the ternary Mg₂SiO₄-Fe₂SiO₄-Fe₃O₄ [O'Neill *et al.*, 1993]. As mentioned above, samples are loaded in a Pt tube, which absorbs iron from silicates and may form ferric iron in silicates. In order to evaluate this effect on the partition coefficient, we conducted one experiment at 1900 K, in which olivine solid solutions are loaded in an Fe tube that minimizes oxidation of wadsleyite.

3. Results

[24] Results of in situ X-ray diffraction are summarized in Table 1, and results of supplemental experiments are shown in Table 2. Partition coefficients for Fe and Mg between olivine and wadsleyite, $K_{Ol-Wd}^{Fe-Mg} = (X_{Ol}^{Fe}/X_{Wd}^{Fe})/(X_{Ol}^{Mg}/X_{Wd}^{Mg})$, where X_q^p is a fraction of component *p* in phase *q*, at 1900 K are nearly identical (0.60 ~ 0.62) regardless of the compositions of the starting materials or run products. This provides evidence that the run products at 1900 K are

in chemical equilibrium. The partition coefficient obtained from the supplemental experiment under reducing conditions is essentially the same, 0.61. We conclude that the oxidation of silicate by absorption of Fe into a Pt tube is negligible. We have adopted 0.61 for K_{Ol-Wd}^{Fe-Mg} , which is the average of 1900 K runs.

[25] In contrast, K_{Ol-Wd}^{Fe-Mg} at 1600 K shows considerable scatter. Most notably, run 779 has a K_{Ol-Wd}^{Fe-Mg} that is lower than in other runs. The starting compositions in this run were Mg# = 95 and close to pure forsterite. The compositions of coexisting olivine and wadsleyite are very close to each other (Mg# = 98 and 95, respectively). Run durations, which are limited in the synchrotron radiation facility, may be too short to reach chemical equilibrium. The other K_{Ol-Wd}^{Fe-Mg} s at 1600 K agree with each other fairly well. We adopt the average of these runs (0.51) for K_{Ol-Wd}^{Fe-Mg} at 1600 K.

[26] Experimental data points are plotted in Figure 3. The transition pressures have been determined at a precision of better than 0.2 GPa. The binary loops are fairly straight, and do not curve upward, as suggested by Helffrich and Wood [1996]. There is an indication that the loops actually curve slightly downward, but the precision and compositional range are not sufficient to resolve the curvature.

[27] Stixrude [1997] proposed a formalism for expressing a binary phase loop. Parameters of this formalism are transition pressures of end-members Mg₂SiO₄ and hypothetical Fe₂SiO₄ and the partition coefficient K_{Ol-Wd}^{Fe-Mg} . Experimental results at 1600 and 1900 K are reproduced using the partition coefficients mentioned above at transition pressures of 14.15 and 15.35 GPa for Mg₂SiO₄ and 5.9 and 7.2 GPa for Fe₂SiO₄ at 1600 and 1900 K, respectively. Thus the temperature dependence of the transition pressure in Mg₂SiO₄ is fairly large at 4.0 MPa/K. The binary loops generated following Stixrude's [1997] formalism are also shown in Figure 3. The transition pressures of the hypothetical end-member of Fe₂SiO₄ at 1900 K estimated in this study are lower than the pressures of olivine-spinel transition in Fe₂SiO₄ that is estimated by extrapolation of the phase boundary given by Yagi *et al.* [1987]. If the stability field of Fe₂SiO₄ wadsleyite does not exist, pressure of the

Table 2. Results of Supplemental Experiments

<i>T</i> , K	Duration, min	Mg# _{Ol}	Mg# _{Wd}	<i>K</i>
1600	60	88.3 (6)	78.9 (7)	0.50 (4)
1600	130	94.2 (5)	88.6 (7)	0.48 (5)
1600	86	90.7 (6)	84.4 (1)	0.56 (6)
1900 ^a	5	79.8 (4)	70.5 (5)	0.60 (3)

^aThe run at 1900 K was conducted using a Fe capsule.

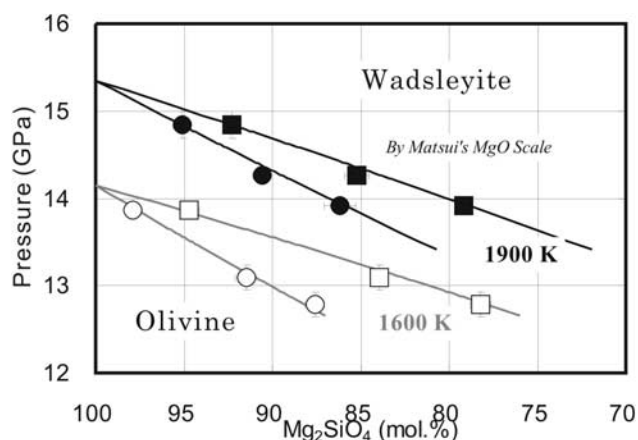


Figure 3. Experimental result and phase relations of the olivine-wadsleyite transition in the system $(\text{Mg,Fe})_2\text{SiO}_4$ at 1600 and 1900 K. The binary loops are drawn using the formalism of *Stixrude* [1997].

hypothetical olivine-wadsleyite transition in Fe_2SiO_4 must be lower than that of the olivine-ringwoodite transition. It is possible that the wadsleyite solid solution may have fairly large nonideality, especially in the Fe-rich side. The possible downward curvatures of the loops might be due to this nonideality. It is also possible that narrow stability field of Fe_2SiO_4 wadsleyite may exist at high temperatures, although *Ohtani* [1979] did not show presence of Fe_2SiO_4 wadsleyite near the melting curve of Fe_2SiO_4 .

4. Discussion

4.1. Comparison With Previous Work

[28] Pressures of the olivine-wadsleyite transition in Mg_2SiO_4 are plotted against temperature in Figure 4, and are compared to results from previous studies [*Katsura and Ito*, 1989; *Akaogi et al.*, 1989; *Morishima et al.*, 1994]. The transition pressures obtained in the present and previous studies are generally consistent in the temperature range investigated (1600 and 1900 K). In particular, results from the present study and *Morishima et al.* [1994], both of which are in situ X-ray diffraction studies, are in excellent agreement. *Morishima et al.* [1994] used NaCl as a pressure standard with the Decker scale [*Decker*, 1971], in contrast to the Matsui's MgO scale in this study. The excellent agreement of the phase boundaries obtained using Matsui's MgO and Decker's NaCl scales implies reliability of these two pressure scales.

[29] The quench experiments of *Katsura and Ito* [1989] gave a Clapeyron slope of 2.5 MPa/K, which is significantly smaller than those obtained by in situ X-ray diffraction (this study: 4.0 MPa/K, *Morishima et al.* [1994]: 3.6 MPa/K). Apparently, the quench experiments yield less positive and more negative Clapeyron slope than in situ X-ray diffraction studies. For example, *Suzuki et al.* [2000] determined the phase boundary of the wadsleyite-ringwoodite transition in Mg_2SiO_4 by in situ X-ray diffraction, and gave a Clapeyron slope of 6.9 MPa/K. In contrast, the Clapeyron slope determined from the quench results of *Katsura and Ito* [1989] is 5 MPa/K. *Katsura et al.* [2003] studied the phase boundary of the postspinel transition in Mg_2SiO_4 , and

showed that the lower bound of the Clapeyron slope is -2.0 MPa/K. Again, the Clapeyron slope determined from the quench experiments [*Ito and Takahashi*, 1989] is -3 MPa/K. This tendency implies that pressure drops at high temperature may be systematically overestimated in quench experiments.

[30] The phase boundary calculated thermochemically by *Akaogi et al.* [1989] also showed a less steep Clapeyron slope than obtained in the present study. The estimation of volumes of olivine and wadsleyite are considered to be relatively reliable, and therefore, the estimation of entropies, especially of wadsleyite, may have significant errors.

[31] The binary loop of the olivine-wadsleyite transition in $(\text{Mg,Fe})_2\text{SiO}_4$ at 1900 K obtained in this and previous studies [*Katsura and Ito*, 1989; *Akaogi et al.*, 1989] are plotted in Figure 5. The transition pressure of the end-member estimated by *Katsura and Ito* [1989] is somewhat lower than in the present study. This is probably a result of imprecise estimation of experimental pressure by *Katsura and Ito* [1989]. The loop thermochemically calculated by *Akaogi et al.* [1989] also has a lower transition pressure. It is very difficult to obtain wadsleyite with composition of $\text{Mg\#} < 80$, and therefore, knowledge of thermochemical properties of Fe_2SiO_4 wadsleyite is very limited. Calculation of the olivine-wadsleyite binary loop based on thermochemical data is certainly problematic.

[32] The partition coefficients $K_{\text{Ol-Wd}}^{\text{Fe-Mg}}$ given by *Katsura and Ito* [1989] are in the ranges from 0.54 to 0.62 and from 0.40 to 0.52 at 1873 and 1473 K, respectively. Thus the $K_{\text{Ol-Wd}}^{\text{Fe-Mg}}$ given in this study generally agree with those given by our previous study. *Fei and Bertka* [1999] determined $K_{\text{Ol-Wd}}^{\text{Fe-Mg}}$ at 1673 K, and showed that $K_{\text{Ol-Wd}}^{\text{Fe-Mg}}$ ranges from 0.45 to 0.51 with increasing Mg content. $K_{\text{Ol-Wd}}^{\text{Fe-Mg}}$ at 1673 K is estimated to be 0.53 from the present results. Although these two studies show fairly consistent results, $K_{\text{Ol-Wd}}^{\text{Fe-Mg}}$ given in this study is slightly closer to unity than those by *Fei and Bertka* [1999]. If this is because temperature difference, temperatures in this study is 50–70 K higher than those in

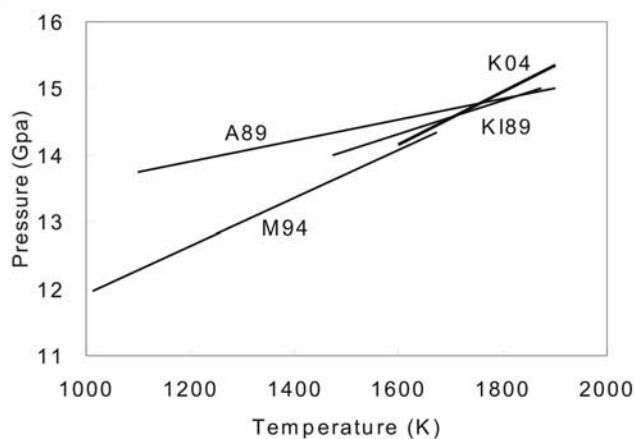


Figure 4. Transition pressures of the olivine-wadsleyite transition in Mg_2SiO_4 versus temperature. The thick line is that obtained in this study, and the other lines are from previous studies: K04, this study; KI89, *Katsura and Ito* [1989]; A89, *Akaogi et al.* [1989]; and M94, *Morishima et al.* [1994].

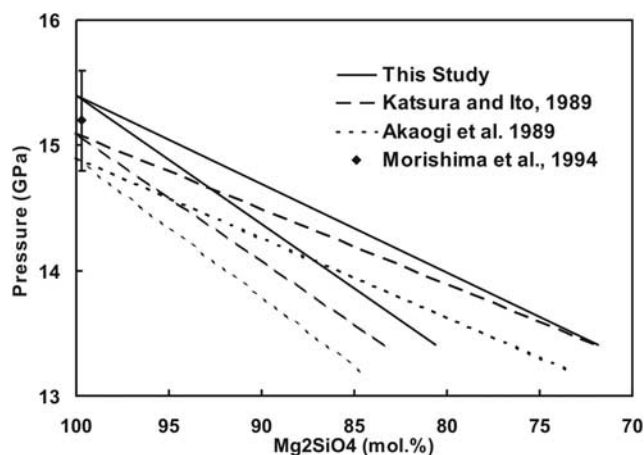


Figure 5. Comparison of the binary loop of the olivine-wadsleyite transition in $(\text{Mg,Fe})_2\text{SO}_4$ at 1900 K from different studies: solid line, this study; dashed line, Katsura and Ito [1989]; and dotted line, Akaogi et al. [1989].

Fei and Bertka [1999]. The discrepancy could be due to the difference of oxidation conditions: Oxidation conditions of the sample with Mo and Re in Fei and Bertka [1999] might be higher than those with BN, which is a reducing material, in this study.

4.2. Temperature at the 410 km Discontinuity

[33] The olivine-wadsleyite transition pressure has large temperature dependence of 4 MPa/K and, therefore, we can estimate temperature at the discontinuity by comparing the depth of the discontinuity with the pressures of the olivine-wadsleyite transition. In the following discussion, we assume that the upper mantle has a pyrolitic bulk composition with a bulk Mg# of about 89 [e.g., McDonough and Sun, 1995]. In addition, we regard the point where the ratio of wadsleyite to olivine is 2:1 corresponds to the reflection plain of the 410 km discontinuity [Stixrude, 1997]. Using these assumptions, the transition pressure is 13.4 GPa (400 km) and 14.5 GPa (430 km) at 1600 and 1900 K, respectively. Therefore the rate of change of the depth of the discontinuity with increasing temperature is 0.1 km/K.

[34] Recently, global mapping of the depth of the 410 km discontinuity has become available [Gu et al., 1998; Flanagan and Shearer, 1998, 1999]. Global averages for the depth of the discontinuity are 411 and 418 km as given by Gu et al. [1998] and Flanagan and Shearer [1998, 1999], respectively. On the basis of our phase relations, these depths correspond to 1710 and 1780 K, respectively. Revenaugh and Jordan [1991] suggested that the average depth of the discontinuity in western Pacific is 414 km, which implies a temperature of 1740 K at the discontinuity. Taking all these estimates into account, the average temperature at the 410 km discontinuity is 1740 ± 35 K for a pyrolitic mantle.

[35] The Speziale EoS for MgO gives $0.15 \sim 0.17$ GPa lower pressures than the Matsui scale. As a result, the estimated temperature at the discontinuity becomes 40 K higher when using the Speziale scale. Factoring in the difference in transition pressure given by these two EoSs,

the temperature at the discontinuity is estimated to be 1760 ± 45 K.

[36] It is also possible to estimate local temperatures. Collier and Helffrich [1997] studied the depth of the 410 and 660 km discontinuity in and near the Izu-Bonin slab. They demonstrated that the depth of the 410 km discontinuity is elevated to 350 km depth in that slab. If the phase transition occurs under equilibrium conditions, the temperature in the Izu-Bonin slab will be 1100 K at the discontinuity. If metastable olivine is subducted to the deeper regions than the equilibrium boundary because of the sluggish kinetics, the temperature in this region should be lower than the above temperature.

4.3. Mantle Geotherm

[37] The mantle geotherm can be estimated by assuming an adiabatic temperature gradient. If no phase transition occurs, the adiabatic geotherm $(dT/dz)_s$ is expressed as

$$(dT/dz)_s = \alpha g T / C_p, \quad (1)$$

where α is the thermal expansion coefficient, g is the gravity constant, T is temperature, and C_p is heat capacity at constant pressure. The thermal expansion coefficients and heat capacities of mantle minerals at ambient pressure and high temperatures are taken from the summaries given by Akaogi et al. [1989, 1998].

[38] Although the gravity constant and heat capacity do not change much through the mantle, the thermal expansion coefficient is believed to decrease considerably with increasing depth [Anderson, 1967]. The ratio of the thermal expansion coefficient at high pressure to that at ambient pressure, α_0 , is usually expressed as a function of compression at ambient temperature, V/V_0 :

$$(\alpha/\alpha_0) = (V/V_0)^{\delta_T}. \quad (2)$$

The constant δ_T is called the Anderson-Grüneisen parameter. Appropriate values of this parameter for mantle minerals are not well determined. Anderson and Isaak [1995] suggest that this parameter is from 4 to 6 for mantle minerals. Chopelas and Boehler [1992] suggested a value of 5.5. The dilatations of periclase calculated by Matsui et al. [2000] imply that this parameter is 4.6. For estimating temperature in the upper mantle, we use a value of 5 for δ_T .

[39] If a phase transition occurs, the geotherm will be deflected due to latent heat associated with the transition at adiabatic conditions. The temperature change due to the latent heat ΔT_{latent} is calculated from

$$\Delta T_{\text{latent}} = \frac{T \Delta V (dP/dT)_{\text{trans}}}{C_p}, \quad (3)$$

where $(dP/dT)_{\text{trans}}$ is the Clapeyron slope of the transition and ΔV is the volume change associated with the transition. The ΔV s are calculated from thermoelastic data summarized by Akaogi et al. [1989, 1998]. The $(dP/dT)_{\text{trans}}$ and ΔV for the olivine-wadsleyite transition are 3.7 MPa/K for Mg# = 89 and $-2.09 \times 10^{-6} \text{ m}^3$, and ΔT is found to be 60 K. On the basis of the assumptions discussed in the beginning of section 4.5, the geotherm will increase by 40 and 20 K above and below the 410 km discontinuity,

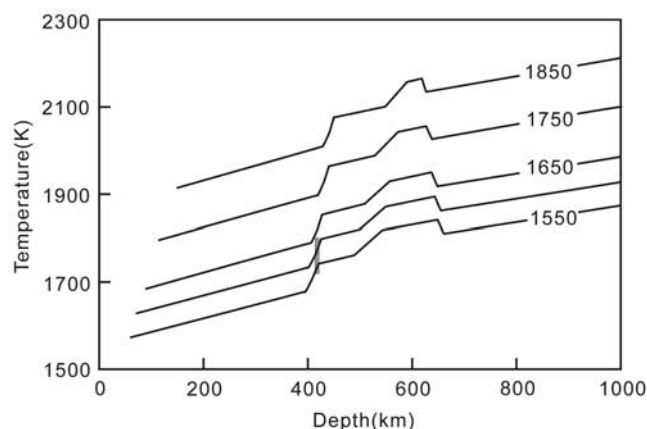


Figure 6. Adiabatic geotherms in the upper mantle with various potential temperatures. The temperatures inferred from the depth of the 410 km discontinuity (the shaded rectangle) suggest a potential temperature of 1530–1620 K.

respectively. The $(dP/dT)_{\text{trans}}$ and ΔV for the wadsleyite-ringwoodite transition are 6.9 MPa/K [Suzuki *et al.*, 2000] and $-0.86 \times 10^{-6} \text{ m}^3$, and the ΔT is found to be 43 K. The $(dP/dT)_{\text{trans}}$ and ΔV for the postspinel transition are -2.0 MPa/K , which is the steepest bound of the range given by Katsura *et al.* [2003], and $-3.02 \times 10^{-6} \text{ m}^3$, and the ΔT is found to be -34 K . The latent heats due to the pyroxene-garnet and garnet-perovskite transitions are small and are neglected.

[40] Calculated geotherms for the upper mantle are shown in Figure 6. Note that the deflections at phase transition boundaries occur due to latent heat effects under the assumption of an adiabatic temperature gradient. The depths of the deflection associated with the wadsleyite-ringwoodite transition are estimated from the phase diagrams given by Katsura and Ito [1989] and Suzuki *et al.* [2000]. The pressures of the postspinel transition have not been well determined using a reliable pressure marker. The recent in situ X-ray diffraction study [Katsura *et al.*, 2003] only suggests only the Clapeyron slope of the post spinel transition in Mg_2SiO_4 (-2 MPa/K). As is shown below, the temperature at the 660 km discontinuity is inferred around at 1900–1870 K. Hence the discontinuity is temporally placed at 1885 K and 660 km, and the depth of the discontinuity is changed with temperature using the Clapeyron slope given by Katsura *et al.* [2003]. Thermal diffusion in the mantle is likely to smear out the temperature change as described below in section 4.5.

[41] On the basis of our analysis of mantle temperature at the 410 km discontinuity, mantle potential temperature (i.e., adiabatically decompressed temperature at the surface) is found to be in the range 1530–1620 K. Mantle potential temperatures below mid-oceanic ridges have been estimated from the composition of MORB [McKenzie and Bickle, 1988], and are predicted to be 1550 K or higher. Thus the geotherm estimated by comparison of the depth of the 410 km discontinuity with the olivine-wadsleyite transition pressure is in excellent agreement with that estimated using MORB.

[42] Temperatures at the bottom of the upper mantle and the top of the lower mantle are found to be 1880 and 1850 K, respectively, with an uncertainty of 50 K. Ito and Katsura

[1989] estimated the temperature at the 660 km discontinuity to be $1870 \pm 100 \text{ K}$. Thus the earlier estimation is in general agreement with the present one. Katsura and Ito [1996] estimated the equilibrium temperature of a diamond inclusion to be 2040 K. This value is substantially higher than the present estimation. One possible explanation for this difference would be that the diamond records the temperature of an ancient geotherm when the mantle had a higher potential temperature, although other reasons can be considered to explain this difference.

[43] The lowermost part of the convection cell of the lower mantle could be calculated, but depends largely on the Anderson-Grüneisen parameter. As this parameter varies from 4 to 6, the estimated temperature ranges from 2190 to 2070 K (Figure 7). Thus the determination of the thermal expansion coefficient at high pressure is essential for accurate estimation of the geotherm in the lower mantle. Combined with the uncertainty in estimating the temperature at the 410 km discontinuity, the temperature at the bottom of the lower mantle is estimated to be 2020–2250 K.

4.4. Topography of the 410 km Discontinuity

[44] Gu *et al.* [1998] showed a global topography map of the 410 km discontinuity based on SS precursors. This map exhibited a depression of the discontinuity under Pacific and Indian Oceans and elevation under continental regions. The average difference in depth is about 5 km. They suggested that the topography of the discontinuity is correlated with the shear velocity anomaly above the discontinuity.

[45] The phase diagram on Figure 3 indicates that a 5 km variation in the depth of the 410 km discontinuity corresponds to variation in temperature of 50 K. High-temperature elasticity of olivine determined by Isaak [1992] suggests that the shear wave velocity has a temperature dependence of about 0.01%/K. Therefore the shear wave velocity should decrease by 1% with elevation of the discontinuity by 10 km. Although it is hard to read the maps quantitatively, the magnitude of variations of the

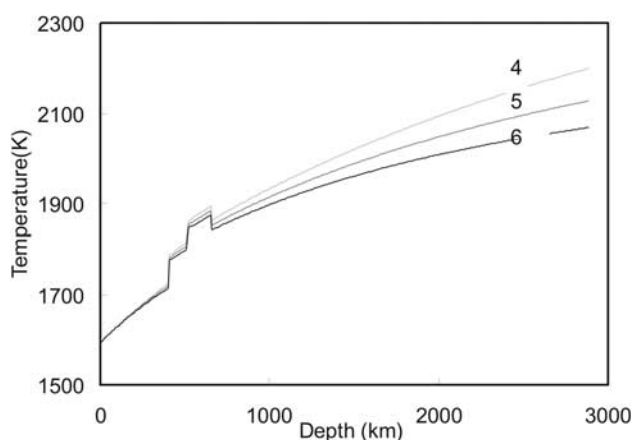


Figure 7. Adiabatic geotherms with a potential temperature of 1590 K. The numbers are assumed Anderson-Grüneisen parameters. The temperature of the lowermost parts of the lower mantle with heat transfer by convection are in the range 2070–2190 K.

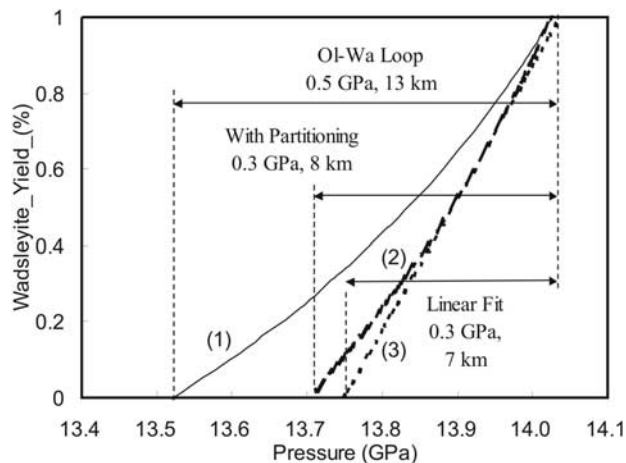


Figure 8. Thickness of the olivine-wadsleyite transition with bulk composition of $Mg\# = 89$. Curve 1 denotes the yielding of wadsleyite with the transition in the pure olivine mantle. Curve 2 denotes that in the pyrolite mantle after taking into account the effect of Fe-Mg partitioning among coexisting mantle minerals. Line 3 is the linear fit to curve 2 at a contact point where the rate of wadsleyite to olivine is 2:1, indicating the effective thickness of the transition for the mantle discontinuity.

discontinuity depth by *Gu et al.* [1998] seems consistent with that of the shear velocity anomaly [*Su et al.*, 1994; *Zhou*, 1996], based on the rate of the correlation mentioned above. Therefore we would estimate that temperatures at the 410 km depth under oceanic regions are about 50 K higher than those under continental regions.

[46] *Flanagan and Shearer* [1998, 1999] also presented global topography maps of the 410 km discontinuity using *SS* and *PP* precursors, respectively. They showed peak-to-peak variation in depth of the 410 km discontinuity of 22 km using *SS* precursors. *Flanagan and Shearer* [1999] showed a 27 km variation using *PP* precursors. Contrary to *Gu et al.* [1998], their topography map exhibit little correlation of discontinuity depth with surface tectonic features; that is, no significant depression and elevation under the oceanic and continental regions, respectively. Instead, maps based on *SS* and *PP* precursors showed depression of the discontinuity under the Pacific Ocean and South America, and elevation under the Indian Ocean and Africa.

[47] Given these results and assuming that the topography of the 410 km discontinuity is caused by temperature variation, lateral variation at the 410 km depth should be about 250 K. Temperatures under the Pacific Ocean would be higher than those under the Indian Ocean, in qualitative agreement with MORB chemistry [e.g., *Klein and Langmuir*, 1987]. If both the topography of the discontinuity and velocity anomaly are caused by temperature variation, these two patterns should be strongly correlated. However, tomographic images [*Su et al.*, 1994; *Zhou*, 1996] have no correlation with the topography maps given by *Flanagan and Shearer* [1998, 1999]. Velocity anomalies near the 410 km depth are strongly correlated to the surface tectonic settings, in contrast to the topography map by *Flanagan and*

Shearer [1998, 1999]. Therefore it is very difficult to consider that both topography of the discontinuity and seismic velocity anomalies are caused by the temperature variation in the upper mantle.

[48] In the olivine-wadsleyite transition model for the 410 km discontinuity, one of the possible ways to form topography along the discontinuity is $Mg\#$ variation. If $Mg\#$ is high, the transition pressure will be elevated (Figure 3). In this case, however, seismic wave velocities will also increase [*Isaak*, 1992]. Therefore topography should correlate with velocity anomalies in the opposite way to temperature variation. Again, the topographical maps given by *Flanagan and Shearer* [1998, 1999] do not show any correlation with velocity anomalies. Neither temperature nor $Mg\#$ variation can account for the topography of the discontinuity.

[49] It is very difficult for us to judge which topography map, that given by *Gu et al.* [1998] or *Flanagan and Shearer* [1998, 1999], is a better representation of reality. *Flanagan and Shearer* [1998] claimed that they made more corrections in producing their topography map than *Gu et al.* [1998], although results given by *Gu et al.* [1998] are more understandable in view of mineral physics data. If *Flanagan and Shearer's* [1998, 1999] results are more accurate, the 410 km discontinuity is not explained by the simple olivine-wadsleyite transition model.

4.5. Sharpness of the 410 km Discontinuity

4.5.1. Phase Equilibrium Constraints of Transition Thickness

[50] In this section, we use the olivine-wadsleyite binary loop to predict the depth interval of the 410 km discontinuity. As in section 3, we use the formalism given by *Stixrude* [1997]. We have estimated the temperature at the 410 km discontinuity to be 1760 K for a pyrolitic upper mantle. In this case, the partition coefficient of Fe and Mg between olivine and wadsleyite is estimated to be 0.55. The pressure interval of the transition in a mantle with Fo89 olivine is found to be 0.5 GPa or 13 km (Figure 8).

[51] However, this thickness will not correspond directly to the thickness of the seismic discontinuity, as several other factors must be considered. First, the compositions of olivine and wadsleyite will not be constant across the boundary because these phases partition Fe and Mg differently among pyroxenes and garnet [*Stixrude*, 1997]. Using the partitioning data given by *Irfune and Isshiki* [1998], we calculate that the thickness of the transition is reduced to 8 km in a pyrolitic bulk composition (curve 2 in Figure 8). Second, there is nonlinearity in the yielding rate of wadsleyite associated with the transition [*Stixrude*, 1997]. Applying the method of *Stixrude* [1997] we find that the effect of nonlinearity on the transition thickness is small. The effective thickness is thus calculated to be 7 km (line 3 in Figure 8). The small effect of nonlinearity on the thickness is partly because the Fe-Mg partition coefficient between olivine and wadsleyite is relatively close to unity (0.55).

[52] A final factor to consider is the effect of latent heat on the transition. The effective thickness of 7 km has been estimated under the assumption of constant temperature. However, as discussed in section 4.3, under adiabatic conditions the temperature increases by 60 K at the 410 km discontinuity due to the latent heat of reaction

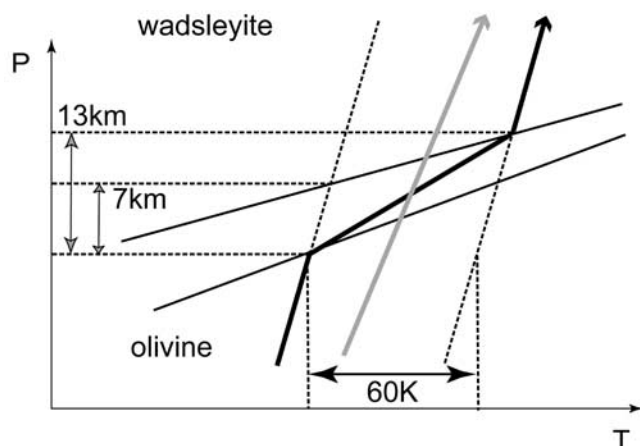


Figure 9. Schematic drawing explaining the effect of the latent heat on the transition width. The upper and lower thin solid lines denote the phase boundaries of olivine to olivine+wadsleyite and olivine+wadsleyite to wadsleyite, respectively. The geotherm increases by 60 K due to the latent heat associated with the olivine-wadsleyite transition (thick black line with an arrow). As a result, the effective thickness is increased from 7 to 13 km. If the flow of the mantle material is sufficiently slow, the kinks of the geotherm disappear due to thermal diffusion (thick gray line with an arrow).

(Figure 6). Because the transition pressure is sensitive to temperature (3.7 MPa/K), the transition interval increases by ~ 6 km in this case (Figure 9). Thus the transition interval could be as large as 13 km in the adiabatic end-member case in which no heat is transferred in the mantle. However, thermal diffusion of heat away from the boundary could effectively smear out the temperature change over a larger depth, so that a 7 km transition thickness represents the other end-member case in which all the latent heat is effectively removed by thermal diffusion.

[53] How slow does movement across the transition have to be for thermal diffusion to be effective? The characteristic distance of thermal diffusion is $\sqrt{\kappa t}$, where κ is thermal diffusivity and t is time. The thermal diffusivity of olivine is around $1 \times 10^{-7} \text{ m}^2/\text{s}$ [Katsura, 1995]. In order for the characteristic distance to be longer than the thickness of the discontinuity by more than one order of magnitude, vertical flow must be slower than 10^{-4} m/yr .

[54] In stagnant regions of the mantle in which vertical movement of material across the transition is very slow or essentially nonexistent, such as is expected over broad regions far from upwelling (e.g., mid-ocean ridges) or downwelling (e.g., subducting slabs) limbs of a convection cell, the transition thickness is expected to approach the value of 7 km. In contrast, in regions of rapid mantle flow the transition thickness should increase and approach a value of 13 km. Thus we predict that systematic variations in transition thickness should be observed in the mantle correlated to tectonic setting.

4.5.2. Seismic Constraints on Transition Thickness

[55] There have been several seismological studies focusing on the sharpness of the 410 km discontinuity. Benz and Vidale [1993] observed a $P'_{410}P'$ phase, which was bounded

beneath the Indian Ocean, in the period range from 0.8 to 2 s. From this observation, they suggested that the thickness of the 410 km discontinuity is less than 4 km and never as thick as 6 km. Yamazaki and Hirahara [1994] observed near-source $p410P$ and $s410P$ phases in the frequency range from 0.2 to 1.0 Hz beneath the Fiji-Tonga region. They suggested that the thickness of the 410 km discontinuity in this region is less than 5 km. Neele [1996] observed that refracted and reflected waves from the 410 km discontinuity occur in a dominant frequency range from 0.4 to 1.5 Hz beneath the Gulf of California. He suggested that most of the velocity increase of the 410 km discontinuity should occur within 4 km. From these observations based on short-period seismic waves, Shearer [2000] concluded that the thickness of the 410 km discontinuity is less than 5 km.

4.5.3. Reconciling Seismic, Phase Equilibrium, and Mineral Physics Observations

[56] Taking all factors into account, our phase relations indicate that at 1760 K in a pyrolitic mantle the depth interval of the olivine-wadsleyite transition should be in the range 7–13 km, which is significantly larger than most seismic observations. Thus the sharpness of the 410 km discontinuity is difficult to explain in view of a pyrolitic mantle model.

[57] Models for bulk silicate Earth and primitive upper mantle are based primarily on mantle xenoliths collected from the upper 200 km in the mantle [e.g., McDonough and Sun, 1995]. In general, there is a commonality among model compositions in that Mg# is about 89, and refractory lithophile major element ratios are near-chondritic, with the notable exception of Mg/Si. The Mg/Si ratio in model primitive upper mantle compositions is generally 15–20% greater than chondritic, and this ratio is reflected directly in the bulk olivine content; the higher the Mg/Si ratio the greater the olivine content. Rather than resorting to difficult to defend, gross changes in chemical and mineralogic

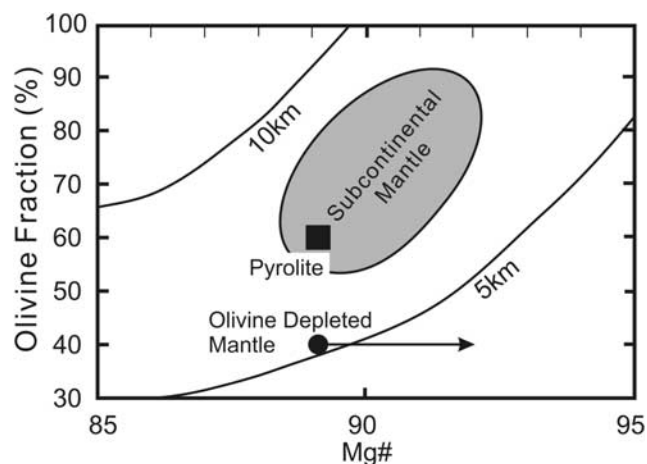


Figure 10. The effective thickness of the olivine-wadsleyite transition as a function of Mg# and olivine fraction in the upper mantle. Pyrolite composition and mantle xenolith are located away from the curves with the effective thickness of 5 km, as indicated by seismic observations. A olivine-depleted mantle gives better agreement with the seismic constraint than does the pyrolitic mantle.

composition in the upper mantle at the 410 km discontinuity, we will now explore how modification of model primitive peridotite composition effects the sharpness of the 410 km discontinuity.

[58] Mantle Mg# and olivine content are critical compositional parameters that affect the transition interval. With increasing Mg#, the interval becomes smaller (Figure 3). With decreasing olivine content, olivine and wadsleyite, respectively, become more Mg-rich and Fe-rich at a constant bulk Mg#. As a result, the transition interval becomes smaller. In Figure 10, the effective thickness of the transition at constant temperature is contoured on the Mg#-olivine content plane.

[59] Figure 10 illustrates that a fertile pyrolitic model upper mantle composition does not satisfy the seismological constraint that the thickness of the 410 km discontinuity is less than 5 km. A possible explanation could be that the mantle is more depleted in basaltic components at depth and has a higher Mg#. However, melt depletion from pyrolite also increases the olivine content. For example, the compositional trend for subcontinental lithosphere is shown on Figure 10, and exhibits a positive correlation between Mg# and olivine content that is presumably due primarily to melt extraction. The effective thickness of the discontinuity is generally constant at 7 ~ 8 km along this trend. Thus direct samples from the uppermost mantle have compositions that cannot account for a 5 km transition thickness, even at high Mg#.

[60] Another possible explanation is that the upper mantle in the region of the 410 km discontinuity is depleted in olivine relative to the uppermost mantle, perhaps with a Mg/Si ratio that corresponds more closely to a chondritic ratio. Depletion in olivine is also consistent with mineral physics constraints. *Duffy et al.* [1995] and *Li et al.* [1998] have measured elastic moduli of wadsleyite at high *P-T* conditions, and both studies indicate that the P wave velocity jump of the 410 km discontinuity is ~40% of that associated with the olivine-wadsleyite transition. If it is assumed that the magnitude of the velocity jump is directly proportional to the olivine content, the elasticity data indicate a mantle with ~40% of olivine.

[61] Figure 10 shows that for a mantle composition with 40% olivine and an Mg# at least 89, the discontinuity is about 5 km or less, assuming no effect of latent heat. Thus two independent lines of evidence from phase equilibrium and mineral physics data support a model mantle composition with ~40% olivine.

[62] Reconciling a mantle with lower Mg/Si at the 410 km discontinuity with the Mg/Si in the uppermost mantle as sampled by xenoliths requires a considerable modification of the standard petrologic mantle model. It is conceivable that the upper mantle inherited the high Mg/Si ratio by flotation of olivine into the uppermost mantle during cooling of a magma ocean, leaving the mantle transition zone depleted in olivine. However, it is difficult to reconcile such a model with the near-chondritic Ni/Co, Mg/Ni and Mg/Co ratios in samples from upper mantle [*McDonough and Sun*, 1995], ratios that would become fractionated from the chondritic value by olivine accumulation. It is also difficult to conceive of how distinct compositional domains or even a compositional gradation could have survived over 4 billion years of convection in the mantle.

[63] Before accepting that the mantle at 410 km has a distinct composition from the uppermost mantle as sampled by xenoliths, it is prudent to look more closely at the seismic constraints. Not all seismic data are consistent with a <5 km thick discontinuity. For example, in their study on the 410 km discontinuity thickness, *Benz and Vidale* [1993] clearly observed a short period $P'_{410}P'$ phase from one event beneath South America. However, they did not observe any $P'_{410}P'$ signal from another event from a similar region. Further, *Xu et al.* [1998] observed $P'_{410}P'_{df}$ with periods near 1.5 and 3.5 s, and showed that the thickness of the 410 km discontinuity beneath south Africa is from 9 to 20 km, values more consistent with the phase relations. They suggested that the thickness of the 410 km discontinuity might vary on a global scale.

[64] As for the magnitude of the velocity jump, *Shearer* [2000] suggested that reported P wave velocity jumps at the 410 km discontinuity are quite scattered and in the range from 4 to 8%. Values at the higher end of this range are consistent with a pyrolitic mantle composition. In addition, the global models, preliminary reference Earth model (PREM) [*Dziewonski and Anderson*, 1981] and iasp91 [*Kennet and Engdahl*, 1991], show significantly smaller magnitude of the discontinuity than the local models. Therefore it is difficult to estimate the average olivine content by comparing the magnitude of the discontinuity with the velocity change associated with the transition.

[65] At present we cannot uniquely account for the apparent discrepancy between seismic data that predicts a transition thickness less than 5 km and our phase equilibrium data which constrains the thickness to be >7 km in a pyrolitic mantle. At this point, we are content to point out the contradiction, and suggest that a mantle depleted in olivine relative to the uppermost mantle is one way to reconcile the observations.

[66] We have also made the prediction from phase relations that the transition thickness should change with tectonic region according to the rate of material flow across the boundary. An obvious test case is to look at regions of subduction, as slabs are estimated to subduct at a rate on the order of $10^{-3} \sim 10^{-2}$ m/yr. Hence the thickness of the transition should be less sharp in and near subducting slabs. However, *Yamazaki and Hirahara* [1994] observed short-period $p410P$ and $s410P$ phases near the Fiji-Tonga slab, indicating a thin transition as in other regions of the mantle. In order to reconcile this observation with phase equilibrium data again requires a mantle and slab component with low olivine content or high Mg#.

[67] In order to ultimately resolve these apparent contradictions between phase relations and seismic observation regarding the transition thickness, detailed seismic mapping of the 410 km discontinuity is required.

5. Conclusions

[68] We have determined phase relations of the olivine-wadsleyite transition in the system $(\text{Mg,Fe})_2\text{SiO}_4$ at 1600 and 1900 K using the quench method with pressure determination by in situ X-ray diffraction using an MgO pressure standard. In this way, experimental pressures were determined at a precision better than 0.2 GPa, permitting the most precise determination of phase relations to date.

[69] Phase relations are generally consistent with the previous results. However, the Clapeyron slope of the olivine-wadsleyite transition is found to be much steeper (4 MPa/K) than previously obtained by the conventional quench method [Katsura and Ito, 1989] and thermochemical calculation [Akaogi et al., 1989]. Also, the binary loops in the pressure-composition plane were found to be steeper than obtained previously. In the investigated compositional range, the binary loops do not have the crescent shape.

[70] The average temperature at 410 km discontinuity is estimated by comparing the transition pressure with the depth of the discontinuity for an upper mantle with a pyrolitic bulk composition. By taking into account the uncertainty of the depth of the discontinuity and transition pressure, the average temperature is found to be 1760 ± 45 K. This temperature range implies that the mantle potential temperature is in the range from 1530 to 1620 K, which is consistent with estimates based on MORB chemistry. The temperature at the bottom of the upper and lower mantle would be 1810–1910 K and 2020–2250 K, respectively.

[71] If it is assumed that topography on the 410 km discontinuity is caused by a temperature variation on the order of 250 K is implied. However, the velocity anomalies obtained from mantle tomography, which are also believed to be caused by temperature variation, show quite different patterns with the discontinuity topography and, therefore, it is difficult to argue for such large temperature variation in the upper mantle.

[72] At a constant temperature of 1760 K, the interval of the olivine-wadsleyite transition in a pure Fo89 olivine mantle is found to be 13 km. Taking into account the effects of Fe-Mg partitioning among coexisting phases as well as nonlinear transition rate, the effective thickness of the transition is about 7 km. The effect of latent heat on the transition could increase this thickness to as much as 13 km under adiabatic conditions. Thus the thickness depends on the efficiency of heat transfer away from the boundary. In regions of rapid mantle flow across the transitions, such as in regions of convective upwelling or downwelling, the transition should be thicker than in stagnant regions where thermal diffusion can smear out the effect of latent heat.

[73] Several seismic observations using short-period reflected and converted phases indicate a transition interval less than 5 km. This discrepancy is difficult to reconcile with a pyrolitic upper mantle composition. An upper mantle containing ~40% olivine with Mg# of 89 could be consistent with a thin discontinuity. Upper mantle with this olivine content is also required to account for the velocity jumps at the 410 km discontinuity. An olivine depleted mantle in the region of the 410 km discontinuity would require a considerable shift in the standard petrologic model for the upper mantle. However, we have to note that even though we accept a chondritic mantle, the short-period reflection and conversion waves near the subducted slab cannot be explained.

[74] In order to resolve the apparent discrepancy among seismic observations and phase equilibrium data, resolution of the issue of transition thickness will require detailed seismic mapping of the 410 km discontinuity. Especially critical is a systematic study searching for a correlation between transition thickness and tectonic environment, as our phase equilibrium data indicates that in regions of rapid

mantle flow, the transition could be nearly twice the thickness as in regions of stagnant mantle.

[75] **Acknowledgments.** We thank C. Oka and Y. Shimizu for their technical assistance. In situ X-ray diffraction experiments were conducted at the synchrotron radiation facility SPring-8 (proposal numbers 1998A0036-ND-np, 1998A0233-ND-np, 2000A0373-ND-np, 2000B0404-ND-np, 2001A0289-ND-np, and 2001B0188-CD-np).

References

- Akaogi, M., E. Ito, and A. Navrotsky (1989), The Olivine-modified spinel-spinel transitions in the system $\text{Mg}_2\text{SiO}_4\text{-Fe}_2\text{SiO}_4$: Calorimetric measurements, thermochemical calculation, and geophysical application, *J. Geophys. Res.*, **94**, 15,671–15,685.
- Akaogi, M., H. Kojitani, K. Matsuzaka, and T. Suzuki (1998), Postspinel transformations in the system $\text{Mg}_2\text{SiO}_4\text{-Fe}_2\text{SiO}_4$: Element partitioning, calorimetry, and thermodynamic calculation, in *Properties of Earth and Planetary Materials at High Pressure and Temperature*, *Geophys. Monogr. Ser.*, vol. 101, edited by M. H. Manghnani and T. Yagi, pp. 373–384, AGU, Washington, D. C.
- Anderson, O. L. (1967), Equation for thermal expansivity in planetary interiors, *J. Geophys. Res.*, **72**, 3661–3668.
- Anderson, O. L., and D. G. Isaak (1995), Elastic constants of mantle minerals at high temperature, in *Mineral Physics and Crystallography: A Handbook of Physical Constants*, *AGU Ref. Shelf*, vol. 2, edited by T. J. Ahrens, pp. 64–96, AGU, Washington, D. C.
- Anderson, O. L., D. G. Isaak, and S. Yamamoto (1989), Anharmonicity and the equation of state for gold, *J. Appl. Phys.*, **65**, 1534–1543.
- Benz, H. M., and J. E. Vidale (1993), Sharpness of upper-mantle discontinuities determined from high-frequency reflections, *Nature*, **365**, 147–150.
- Chopelas, A., and R. Boehler (1992), Thermal expansivity in the lower mantle, *Geophys. Res. Lett.*, **19**, 1983–1986.
- Collier, J. D., and G. R. Helffrich (1997), Topography of the “410” and “660” km seismic discontinuities in the Izu-Bonin subduction zone, *Geophys. Res. Lett.*, **24**, 1535–1538.
- Decker, D. L. (1971), High-pressure equation of state for NaCl, KCl, and CsCl, *J. Appl. Phys.*, **42**, 3239–3244.
- Duffy, T. S., C.-S. Zha, R. T. Downs, H.-K. Mao, and R. J. Hemley (1995), Elasticity of forsterite to 16 GPa and the composition of the upper mantle, *Nature*, **378**, 170–173.
- Dziewonski, A. M., and D. L. Anderson (1981), Preliminary reference Earth model, *Phys. Earth Planet. Inter.*, **25**, 297–356.
- Fei, Y., and C. M. Bertka (1999), Phase transitions in the Earth’s mantle and mantle mineralogy, in *Mantle Petrology: Field Observations and High Pressure Experimentation*, edited by Y. Fei, C. M. Bertka, and B. O. Mysen, *Spec. Publ.* 6, pp. 189–207, Geochem. Soc., Houston, Tex.
- Flanagan, M. P., and P. M. Shearer (1998), Global mapping of topography on transition zone velocity discontinuities by stacking SS precursors, *J. Geophys. Res.*, **103**, 2673–2692.
- Flanagan, M. P., and P. M. Shearer (1999), A map of topography on the 410-km discontinuity from PP precursors, *Geophys. Res. Lett.*, **26**, 549–552.
- Gu, Y., A. M. Dziewonski, and C. B. Agee (1998), Global de-correlation of the topography of transition zone discontinuities, *Earth Planet. Sci. Lett.*, **157**, 57–67.
- Hama, J., and K. Suito (1999), Thermoelastic properties of periclase and magnesio-wuestite under high pressure and high temperature, *Phys. Earth Planet. Inter.*, **114**, 165–179.
- Helffrich, G., and C. R. Bina (1994), Frequency dependence of the visibility and depths of mantle seismic discontinuities, *Geophys. Res. Lett.*, **21**, 2613–2616.
- Helffrich, G. R., and B. J. Wood (1996), 410 km discontinuity sharpness and the form of the olivine α - β phase diagram resolution of apparent seismic contradictions, *Geophys. J. Int.*, **126**, F7–F12.
- Irfune, T., and M. Isshiki (1998), Iron partitioning in a pyrolite mantle and the nature of the 410-km seismic discontinuity, *Nature*, **392**, 702–705.
- Irfune, T., et al. (1998), Postspinel phase boundary in Mg_2SiO_4 determined by in situ X-ray measurement, *Science*, **279**, 1698–1700.
- Isaak, D. G. (1992), High-temperature elasticity of iron-bearing olivines, *J. Geophys. Res.*, **97**, 1871–1885.
- Ito, E., and T. Katsura (1989), A temperature profile of the mantle transition zone, *Geophys. Res. Lett.*, **16**, 425–428.
- Ito, E., and E. Takahashi (1989), Postspinel transformations in the system $\text{Mg}_2\text{SiO}_4\text{-Fe}_2\text{SiO}_4$ and some geophysical implications, *J. Geophys. Res.*, **94**, 10,637–10,646.
- Jamieson, J. C., J. N. Fritz, and M. H. Manghnani (1982), Pressure measurement at high temperature in X-ray diffraction studies: Gold as a

- primary standard, in *High-Pressure Research in Geophysics*, edited by S. Akimoto and M. H. Manghnani, pp. 27–48, Cent. for Acad. Publ., Tokyo.
- Katsura, T. (1995), Thermal diffusivity of olivine under upper mantle conditions, *Geophys. J. Int.*, **122**, 63–69.
- Katsura, T., and E. Ito (1989), The system $\text{Mg}_2\text{SiO}_4\text{-Fe}_2\text{SiO}_4$ at high pressures and temperatures: Precise determination of stabilities of olivine, modified spinel, and spinel, *J. Geophys. Res.*, **94**, 15,663–15,670.
- Katsura, T., and E. Ito (1996), Determination of Fe-Mg partitioning between perovskite and magnesio-wüstite, *Geophys. Res. Lett.*, **23**, 2005–2008.
- Katsura, T., et al. (2003), Post-spinel transition in Mg_2SiO_4 determined by in situ X-ray diffractometry, *Phys. Earth Planet. Inter.*, **136**, 11–24.
- Kenner, B. L. N., and E. R. Engdahl (1991), Travel times for global earthquake location and phase identification, *Geophys. J. Int.*, **105**, 429–465.
- Klein, E. M., and C. H. Langmuir (1987), Global correlations of ocean ridge basalt chemistry with axial depth and crustal thickness, *J. Geophys. Res.*, **92**, 8089–8115.
- Li, B.-S., R. C. Liebermann, and D. J. Weidner (1998), Elastic moduli of wadsleyite ($\beta\text{-Mg}_2\text{SiO}_4$) to 7 gigapascals and 873 kelvins, *Science*, **281**, 675–677.
- Matsui, M., and N. Nishiyama (2002), Comparison between the Au and MgO pressure calibration standards at high temperature, *Geophys. Res. Lett.*, **29**, 1–4.
- Matsui, M., S. C. Parker, and M. Leslie (2000), The MD simulation of the equation of state of MgO: Application as a pressure calibration standard at high temperature and high pressure, *Am. Mineral.*, **85**, 312–316.
- McDonough, W. F., and S.-S. Sun (1995), The composition of the Earth, *Chem. Geol.*, **120**, 223–253.
- McKenzie, D., and M. J. Bickle (1988), The volume and composition of melt generated by extension of the lithosphere, *J. Petrol.*, **29**, 625–679.
- Morishima, H., T. Kato, M. Suto, E. Ohtani, S. Urakawa, W. Utsumi, O. Shimomura, and T. Kikegawa (1994), The phase boundary between α - and $\beta\text{-Mg}_2\text{SiO}_4$ determined by in situ X-ray observation, *Science*, **265**, 1202–1203.
- Neele, F. (1996), Sharp 400-km discontinuity from short-period *P* reflections, *Geophys. Res. Lett.*, **23**, 419–422.
- Ohtani, E. (1979), Melting relations of Fe_2SiO_4 up to about 200 kbar, *J. Phys. Earth*, **27**, 189–208.
- O'Neill, H. S. C., C. A. McCammon, D. Canil, D. C. Rubie, C. R. Ross, and F. Seifert (1993), Mössbauer spectroscopy of mantle transition zone phases and determination of minimum Fe^{3+} content, *Am. Mineral.*, **68**, 456–460.
- Revenaugh, J., and T. H. Jordan (1991), Mantle layering from *ScS* reverberations: 2. The transition zone, *J. Geophys. Res.*, **96**, 19,763–19,780.
- Ringwood, A. E. (1979), *Origin of the Earth and Moon*, 295 pp., Springer-Verlag, New York.
- Shearer, P. M. (2000), Upper mantle seismic discontinuities, in *Earth's Deep Interior: Mineral Physics and Tomography From the Atomic to Global Scale*, *Geophys. Monogr. Ser.*, vol. 117, edited by S. Karato et al., pp. 115–131, AGU, Washington, D. C.
- Speziale, S., C.-S. Zha, T. S. Duffy, R. J. Hemley, and H.-K. Mao (2001), Quasi-hydrostatic compression of magnesium oxide to 52 GPa: Implications for the pressure-volume-temperature equation of state, *J. Geophys. Res.*, **106**, 515–528.
- Stixrude, L. (1997), Structure and sharpness of phase transitions and mantle discontinuities, *J. Geophys. Res.*, **102**, 14,835–14,852.
- Su, W., R. L. Woodward, and A. M. Dziewonski (1994), Degree 12 model of shear velocity heterogeneity in the mantle, *J. Geophys. Res.*, **99**, 6945–6980.
- Suzuki, A., E. Ohtani, H. Morishima, T. Kubo, Y. Kanbe, T. Kondo, T. Okada, H. Terasaki, T. Kato, and T. Kikegawa (2000), In situ determination of the phase boundary between wadsleyite and ringwoodite in Mg_2SiO_4 , *Geophys. Res. Lett.*, **27**, 803–806.
- Suzuki, I. (1975), Thermal expansion of periclase and olivine, and their anharmonic properties, *J. Phys. Earth*, **23**, 145–159.
- Utsumi, U., K. Funakoshi, S. Urakawa, M. Yamakata, K. Tsuji, H. Konishi, and O. Shimomura (1998), Spring-8 beamlines for high pressure science with multi-anvil apparatus, *Rev. High Press. Sci. Technol.*, **7**, 1484–1486.
- Xu, F., J. E. Vidale, P. S. Earle, and H. M. Benz (1998), Mantle discontinuities under southern Africa from precursors to P' P'_{df} , *Geophys. Res. Lett.*, **25**, 571–574.
- Yagi, T., M. Akaogi, O. Shimomura, T. Suzuki, and S.-I. Akimoto (1987), In situ observation of the olivine-spinel phase transformation in Fe_2SiO_4 using synchrotron radiation, *J. Geophys. Res.*, **92**, 6207–6213.
- Yamazaki, A., and K. Hirahara (1994), The thickness of upper mantle discontinuities, as inferred from short-period J-Array data, *Geophys. Res. Lett.*, **21**, 1811–1814.
- Zhou, H. (1996), A high-resolution *P* wave model for the top 1200 km of the mantle, *J. Geophys. Res.*, **101**, 27,791–27,810.

Y. Aizawa, E. Ito, T. Katsura, M. Song, M. J. Walter, and S. Yokoshi, Institute for Study of the Earth's Interior, Okayama University, Misasa, Tottori-ken 682-0193, Japan. (aizawa@misasa.okayama-u.ac.jp; eito@misasa.okayama-u.ac.jp; tkatsura@misasa.okayama-u.ac.jp; song@misasa.okayama-u.ac.jp; walter@misasa.okayama-u.ac.jp; sho@misasa.okayama-u.ac.jp)

K.-i. Funakoshi, Japan Synchrotron Radiation Research Institute, Kouto 1-1-1, Mikazuki-cho, Sayo-gun, Hyogo 678-5198, Japan. (funakosi@spring8.or.jp)

A. Kubo, Department of Geosciences, Guyot hall, Princeton University, Princeton, NJ 08544, USA. (akubo@princeton.edu)

O. Nishikawa, Department of Earth Sciences, Faculty of Science, Kanazawa University, Kakuma-machi, Kanazawa 920-1192, Japan. (nisikawa@earth.s.kanazawa-u.ac.jp)

T. Shinmei, Geodynamics Research Center, Ehime University, 2-5 Bunkyo-cho, Matsuyama 790-8577, Japan. (shinmei@sci.ehime-u.ac.jp)

H. Yamada, City Hall of Nagahama, Takata 12-34, Nagahama 526-8501, Japan. (yamada-hitoshi@city.nagahama.shiga.jp)

T. Yoshino, Department of Earth and Environmental Sciences, Rensselaer Polytechnic Institute, Troy, NY 12180, USA. (yoshta@rpi.edu)